160

PROCEEDINGS

of the

XXXV INTERNATIONAL WINTER MEETING ON NUCLEAR PHYSICS

◊

BORMIO (ITALY) 1997, February 3rd-8th

Ricerca Scientifica ed Educazione Permanente
Supplemento N. 110, 1997

Edited by I. Iori
Dipartimento di Fisica, Università degli Studi di Milano
Via Celoria 16
20133 Milano, Italy

Boiling a nucleus†

E. C. Pollacco[1], J. Brzychczyk[1,3], C. Volant[1], R. Legrain[1],L. Nalpas[1]
D.S. Bracken[2] ,H. Breuer[5], R.G. Korteling[4], K. Kwiatkowski[2],
K.B. Morley[2], E. Renshaw Foxford[2], V.E. Viola[2],N. R. Yoder[2],
J. Gomez del Campo[6] and J. Cugnon[7]

[1] CEA DAPNIA/SPhN, CE Saclay, 91191 Gif-sur-Yvette CEDEX, France.
[2]Dept. of Chem. & IUCF, Indiana Univ., Bloomington, IN47405, USA.
[3]Inst. of Phys., Jagiellonian Univ. 30-059 Krakow, Poland.
[4]Dept. of Chem., Simon Fraser Univ., Burnaby, BC, Canada.
[5]Dept. of Phys., Univ. of Maryland, College Park, MD 20742, USA.
[6]Oak Ridge National Laboratory, Oak Ridge, TN37831,USA.
[7]Univ. de Liège, Inst. de Physique, B-4000 Liège 1, Belgium.

INTRODUCTION

As with a number of papers presented at this XXXV Bormio conference , this study considers how nuclei respond to large amounts of thermal energy. By *large* we have in mind values reaching the total nucleon binding energy, B. By *respond* we refer, for example, to the trajectory that the system traces in a density versus temperature plot[1]. For a nucleus of mass 130 and low excitation energy, $E^* \sim 100$ MeV, the density is constant and the temperature is dissipated entirely by evaporation. With increasing E^*, evaporation yield gradually gives way to fission and then to multifragmentation [2]. Multifragment production is believed to occur once the nucleus reaches low density. The question that is addressed in this work is whether the *evaporative* channel is still present at high E^*. More specifically, we set out to detect events with a single residual heavy fragment, HF, accompanied preferentially with light particles at $E^* \sim B$. and to compare the data with evaporative decay [3]. At such energies multifragment and suedo-fission production are calculated to be dominant [2]. It is therefore conceivable that the *evaporation* chain is modified by the strong presence of the other channels. For example if we suppose that at high temperatures a monopole expansion [4] occurs, then HF could be associated with events with a monopole collapse. Therefore a signature might still persist in the particle emission chain for the events of interest. This work is interesting within the context of ref. 5.

† Experiment performed at the Laboratoire National Saturne, France

Nuclear reactions are of course necessary to form hot nuclei. The principle difficulty that is encountered is to recognise and isolate the dynamics of the heating process from the characteristics related to hot matter. The contribution by Colonna et al. [6,7] addresses this very question for the system under study. Using intranuclear cascade , INC, plus a stochastic one-body approach, SOBA, they show that for an Ag target and ^{3}He projectile for energies up to 4.8 GeV, the nucleus is shape resilient. That is to say, although the nucleus is initially deformed by a moving wake, it very rapidly ($\leq$60 fm/c) regains its original shape. At this time a large fraction of the available energy is thermalised. From these calculations we conclude that after a brief time, where cascade and pre-equilibrium particles are emitted, the system can be represented as a hot nuclear ball with normal density. Through these calculations we justify the use of two step models.

In this work the data are compared to calculations where we couple, event-by-event, an INC calculation [8] to an evaporation code, SIMON, [9]. The INC calculations are stopped at 30 fm/c [7]. At the incident energy of 1.8 GeV the spectrum of E* following the cascade is Maxwellian like with a mean energy of around 300 MeV. The INC code generates events with single HF and light particles (protons, neutrons and π). Also at this incident energy the mass and charge of the HFs are essentially independent of E* and have values of 95 amu and 43 respectively. The mass width is 7 amu (FWHM). The average angular momentum is small ($\sim 20\hbar$). The more recent version of SIMON uses a formalism similar to that of Charity et al. [10]. In all comparisons shown herein the simulated events are filtered by the experimental acceptance and include the same software conditions as imposed on the data. It is important to emphasise that our choice of well established models [3] investigate their validity in limiting cases. This is at the expense of lack of generality and it is of course desirable to have a more open comparisons. Exit channel models like that of Friedman [4] or Botvina et al. [11] have been [12] or are presently being considered.

The present contribution shows that INC+SIMON gives a good description of the data and justifies the use of the model. However it is important to note that they are necessary in the present context to remove or ease the difficulties related to the interpretation of the data. As with heavy ion induced reactions, selected high E* events could have a significant background from different mechanisms, poor experimental phase space coverage and incomplete analysis procedures. With light ions these obstacles are less important mainly because the events arise from a single source of particle production [13]. Also as we have seen, inherently light ions do not allow a strong modification of the nuclear surface[7]. Thus strong dynamic effects are not expected. However contamination could still arise as a result of, for example, the rapid fall in the E* primary spectrum (INC calculation result) coupled to processes like sequential multiple decay of intermediate mass fragments, IMF, (included in SIMON). Therefore special attention is made to include these effects in the simulation to justify the extracted excitation energy.

Experimental Set-Up

The experiment was performed at the Laboratoire National Saturne, France, using ^{3}He beams at 1.8, 3.6 and 4.8 GeV. In this contribution only the lower energy data set will be discussed. The target was ^{nat}Ag of thickness 1.08 mg/cm^2. Briefly the

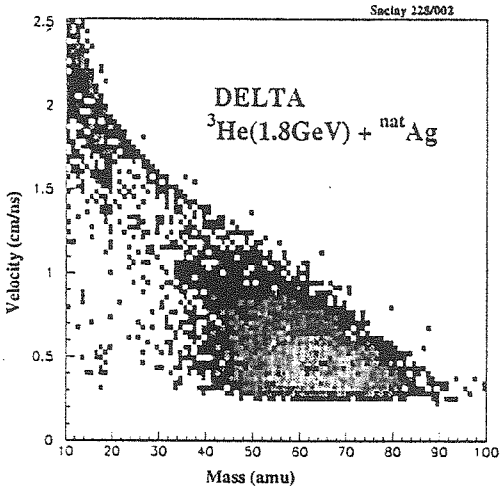

Figure 1. Residual mass versus velocity plot.

experimental set-up consisted of four parts. (i) To measure leading protons ARCOLE was used[14]. This consists of a forward plastic wall made up of 28 fast plastics and mounted so as to have a hole in the centre for the beam. Light from each plastic was read out by two photomultipliers. This assembly covered an angular range of approximately 2.5 to 12° and was positioned to give a minimum flight path from the target of 4 meters. (ii) To detect heavy fragments, HF, a circular hodoscope, DELTA, which included 30 high field Si detectors was used. The target-detector flight path was 60 cm and covered angles between 5 to 10°. (iii) Light charged particles ($Z \leq 2$), LCP, and intermediate mass fragments ($Z \leq 20$), IMF, were detected in an array called ISiS[12,15] which contains 162 triple detector telescopes in a tight geometry. Each telescope is composed of a gas-ionisation chamber, a fully depleted 500μm ion-implanted silicium detector and a 28 mm CsI(Tℓ) crystal. The geometrical acceptance is 70% and thresholds are better than 1 MeV.A. The charge, Z, resolution ranged up to 20. Mass resolution is obtained for those particles which punch through the Si crystal. (iv) An active collimator assembly was employed to vetoe the beam halo particles reaching or stopping in ISiS.

Data Analysis -

Fig. 1 gives the superimposition of 26 mass vs. velocity plots from DELTA for fragments with a minimum trigger of two particles in ISiS. The mass was computed from the time between DELTA - ISiS and energy measurements. Corrections due to time delay[16] and energy defect[17] were included. The latter was achieved through a coincident set-up with slowed down fission fragments in a separate measurement. Velocity thresholds were all better than 0.25 cm/ns. We remark that in light ion

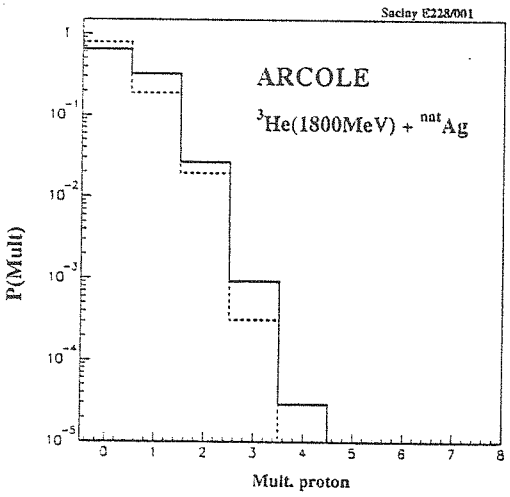

Figure 2. Probability for the multiplicity for high energy protons in the plastic wall ARCOLE with minimum trigger. The dashed histogram refers to the INC+FILTER prediction.

induced reactions it is expected that the highest yield of HF should be for mass values close to that of the target[18]. The shift seen in the figure towards a mean mass of $\sim$ 65 amu is largely due to the target thickness effects and the energy threshold in DELTA. It is important to note, however, that the fragments of interest, the ones below mass 65 amu are not strongly perturbed by the choice of target thickness.

Possibly the only distinct signal of the reaction primordial time that we have captured in our set-up are the fast leading protons under the minimum trigger condition. In fig. 2 we give the overall multiplicity in ARCOLE. The lower energy threshold in ARCOLE is approximately 50 MeV for protons. The dashed histogram gives the filtered multiplicity from the INC calculations and illustrates the reasonable description of the data.

The analysis of the ISiS data was performed by calibration of the ion chambers, Si and CsI channels using alpha sources, precision pulsers and punch through data. This allowed an overlay of practically all 162 telescope two-dimensional spectra. Selection of mass and charge for the light charged particles, and charge for the IMFs were done by drawing appropriate gates. In many respects the calibration is very similar to that given by Kwiatowski et al.[15].

Thermal Energy

The thermal energy of events with a minimum bias in ISiS and which included a HF in DELTA (mass$\leq$ 10 amu) were computed. By *thermal* we refer to the remaining excitation energy after the emission of the pre-equilibrium/cascade particles. Similarly

we refer to thermal mass and charge. To compute the thermal quantities the principal corrections which were introduced are (i) the detector acceptance. This includes the efficiency as a function of charge and mass for low energy particles. The efficiency corrections were established with the aid INC + SIMON and the detector filter. (ii) By far the largest addition to the excitation energy is the contribution of the neutron energy. The mean energy per neutron K_n as a function of E^* was calculated using the code LILITA [19]. An iterative procedure was used. (iii) To obtain the total mass and charge per event, the mass (charge) of the IMFs (HF) was read off from a table of mass versus charge which takes into account the evaporation process. (iv) The thermal quantities were calculated by summing over the particle kinetic energy, mass, charge and Q-values (Q_i) event-by-event. In this analysis the sum was carried over heavy residue and all IMFs. For LCPs the sum was extended over particles with kinetic energies, K_i which are below (25, 32, 39, 54 and 61 MeV) for p, d, t, ^{3}He and ^{4}He respectively. The thermal charge, Z_{th}, gives the total mass, A_{th} by assuming an Z_{th}/A_{th} in the valley of stability. Subtracting the total detected mass from A_{th} gives the number of thermal neutrons, N_n. The energy, E_{th} was calculated by computing the sum $(N_n(K_n+Q_n) + (\Sigma(K_i+Q_i))$ over the thermal particles and corrected for the efficiencies. This analysis shows a constant $A_{th} = 92$ amu with E^* for values greater than 250 MeV and consistent with the INC calculations. Therefore a second and adopted method was also developed where A_{th} and Z_{th} are assumed and given by the INC calculations. In this case the efficiency correction was not employed and the missing mass and charge and corresponding energies were assumed to arise only from LCPs in the same proportion as the detected particles in the event. Performing simulations with the above described procedures shows that the E^* given by INC is well reproduced by the using a constant A_{th}. The efficiency method tends to give large widths in the E_{th} observable.

Results

In fig. 3 a plot is given of the detected heavy mass in DELTA as a function of $\epsilon^* = E_{th}/A_{th}$ with the IMF multiplicity, $M_{IMF} = 0$. We note a number of features. The largest yield is for events with mass of approximately 65. Higher masses are not detected with full efficiency due to the target thickness and energy threshold in DELTA as noted earlier. The island at high excitation $\epsilon^* \sim 9$ A.MeV is not considered here and correspond to events where the HF is not detected in DELTA. The line traced from low to high excitation represents the simulation trend. As shown the data stretch is well reproduced. The rectangle is drawn to have a centre at ϵ^*/B corresponds to 80% . The width and height of the rectangle represent the full width at half maximum for the mass and ϵ^* resolution respectively. The latter value was extracted using the INC+SIMON+FILTER simulation. For events in this region of ϵ^* =6-8 A.MeV the fraction of events with M_{IMF} greater than zero in this region is approximately 25%. These IMFs have charge distribution with a maximum at 3 and decaying very rapidly. This suggests that the loss of mass from the HF by IMF emission is not significant.

Considering the same representation as fig. 3 but with condition M_{IMF}=1 and 2 shows essentially the same data trend but with decreasing statistics and an increasing shift to lower residual mass with M_{IMF} . However no shift to high ϵ^* is remarked. In other words, inclusion of all IMF multiplicities does not change significantly the high

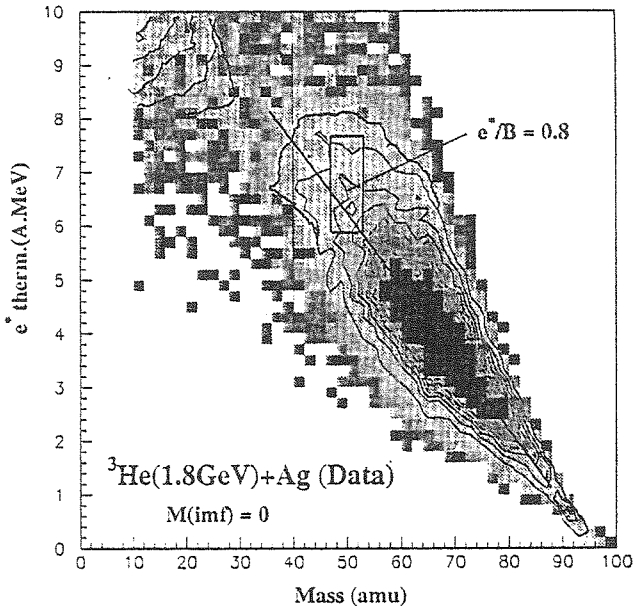

Figure 3. Experimental ϵ^* as a function of residual mass.

part of the ϵ^* spectrum. No higher excitations are obtained by placing higher M_{IMF} windows.

In extracting high excitation events it is interesting, as suggested by in fig. 3 to consider events with low residual masses. The difficulty related to the choice of residual mass window lies with the question of; what is the lowest HF mass and yet still be able to denote it as a residue. And secondly, whether this mass has properties which are consistent with what is expected. Nevertheless, from fig. 3 it is clear that events at high excitation do not exist below 35 amu or so and they are limited to ϵ^* of 8A.MeV. Projecting out the velocity spectra for the heavy masses shows that the range to be considered is 45-50. Below this mass range the velocity spectrum has to be further analysed. Placing a window on the mass and projecting the ϵ^* spectrum gives fig. 4 (solid curve) which has a mean value of ϵ^*/B of 77% . Also given in fig. 4 is the result of the simulation. It shows that the mean is well reproduced as expected. More consequential is that the width of the distribution is well reproduced indicating a good understanding of the underlying processes. Preliminary estimates for the relative yield at these values of ϵ^*/B show to be relatively high.

The HF-coincident Z=2 particle spectra as a function of ϵ^* have been extracted. In fig. 5 the ϵ^* spectra with a window of ϵ^* = 5.5 - 6.5 A.MeV are compared with the INC+SIMON+FILTER calculations. The data shows an evaporative component at low kinetic energy which is well reproduced by the calculations. Beyond 50 MeV the pre-equilibrium process is observed which is, of course not included in the calculations. In fig. 6 a similar comparison is performed for the IMF multiplicity. Again the data, to a large extent, is well reproduced.

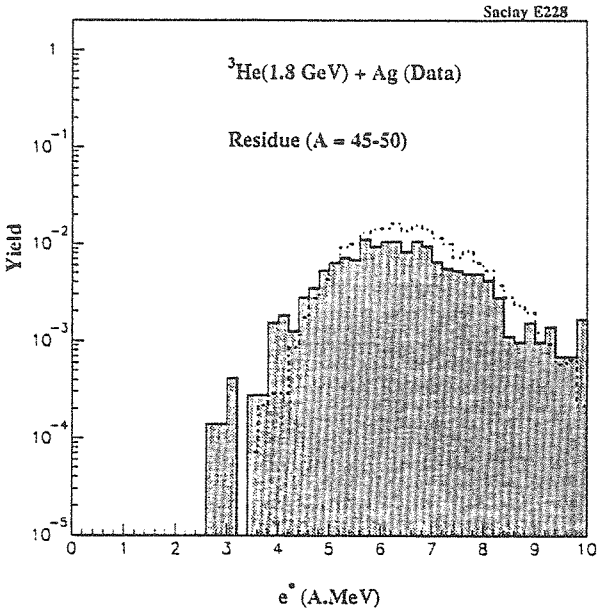

Figure 4. Experimental ϵ^* spectrum with the indicated mass window. The dashed curve represents the simulation.

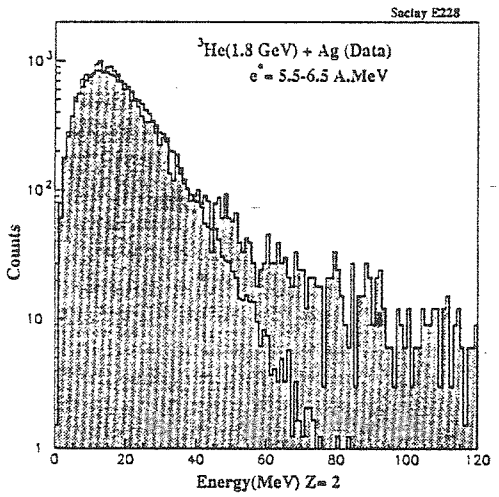

Figure 5. Energy spectrum for Z=2 in coincidence with HF for ϵ^* =5.5 - 6.5MeV/A.

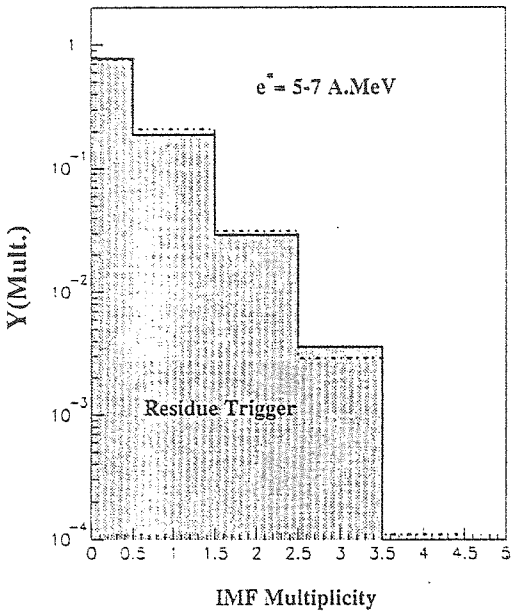

Figure 6. Probability for the IMF multiplicity data (solid histogram). The model predictions are given by the dashed histogram

Conclusion

In conclusion, we report on an experimental study of ^{3}He(1.8 GeV) + Ag where we detected heavy fragments at relatively low velocity in coincidence with LCP and IMFs. The LCP and IMFs were detected in a 4π configuration with low energy threshold. Fast protons are also detected in the forward direction. The global parameters under this configuration are well reproduced with an INC + evaporation description. An attempt is made to extract the highest excitation energy reached for the "evaporation"[2]. Values of ϵ^*/B of 77% are obtained. This energy still leaves a heavy fragment of approximately 47 amu. This ϵ^*/B value corresponds to approximately 22% higher than systematic from heavy ion induced reactions [20]. (It is important to note, however, that the systematic did not use a 4π detection system as performed in this work.) The energy is liberated mostly by light particle emission. The Z=2 spectra and particle multiplicity have an evaporative character which suggests that the system does choose to decay, even at such high excitation energies, through binary decay. The nucleus is made to boil. Further analysis on the 4.8 GeV data and the examination of alternative models is in progress.

REFERENCES

1. V. Viola et al.,Nucl. Dynamics, ed. W. Bauer and G. W. Westfall, Plenum 1996.
2. D. H. E. Gross, Rep. Prog. Phys. 53, 605(1990).
3. L. G. Moretto and G. J. Wozniak, Prog. Part. Nuc. Phys., Vol21.(1988), and ref. therein.
4. W. Friedman, Phys. Rev. C42, 667(1990).
5. S. Levit, P. Bonche, Nucl. Phys. A437, 426(1985).
6. M. Colonna, J. Cugnon and E. C. Pollacco, contribution to this conference.

7. M. Colonna, J. Cugnon and E. C. Pollacco, Phys. Rev. March(1997).
8. J. Cugnon, Nucl. Phys. A462, 751(1987).
9. Modified version of SIMON, D. Durand, Nucl. Phys. A541, 266(1992).
10. R. J. Charity et al., Nucl. Phys. A476, 516 (1988).
11. A. Botvina, A. S. Iljinov and I. Mishustin, Nucl. Phys. A507, 649(1992).
12. K. Kwiatkowski, contribution to this conference.
13. K. B. Morley et al., Phys. Lett. B355, 52(1995).
14. Y. Terrien et al., Phys Lett. B294, 40(1992).
15. K. Kwiatkowski et al., Nucl. Instr. Meth. A360, 5(1995).
16. S.B. Kaufman, et al., Nucl. Instr. Meth. 115, 47(1974).
17. H.O. Neidel, H. Henschel, Nucl. Instr. Meth. 178, 137(1995).
18. S.B. Kaufman and E. P. Steinberg, Phys. Rev. C22, 167(1980)
19. J. Gomez del Campo et al., Phys. Rev. C41 2689(1991)
20. S. Leray, J. de Phys. C4 275(1986).